COHERENCE TRANSITION IN DEGENERATE DIFFUSION EQUATIONS WITH MEAN FIELD COUPLING

KHASHAYAR PAKDAMAN AND XAVIER PELLEGRIN

Abstract. We introduce non-linear diffusion in a classical diffusion advection model with non local aggregative coupling on the circle, that exhibits a transition from an uncoherent state to a coherent one when the coupling strength is increased. We show first that all solutions of the equation converge to the set of equilibria, second that the set of equilibria undergoes a bifurcation representing the transition to coherence when the coupling strength is increased. These two properties are similar to the situation with linear diffusion. Nevertheless nonlinear diffusion alters the transition scenari, which are different when the diffusion is sub-quadratic and when the diffusion is super-quadratic. When the diffusion is super-quadratic, it results in a multistability region that preceeds the pitchfork bifurcation at which the uncoherent equilibrium looses stability. When the diffusion is quadratic the pitchfork bifurcation at the onset of coherence is infinitely degenerate and a disk of equilibria exist for the critical value of the coupling strength. Another impact of nonlinear diffusion is that coherent equilibria become localized when advection is strong enough, a phenomenon that is preculded when the diffusion is linear.

1. Introduction

We consider the equation

$$\begin{cases} \partial_t u &= \partial_\theta^2(u^m) + \partial_\theta\left(uJ * u\right), & t>0,\ \theta\in[0,2\pi],\\ u(0,\theta) &= u_0(\theta) & \theta\in[0,2\pi],\\ u(t,0) &= u(t,2\pi) & t\geq 0,\\ \partial_\theta u(t,0) &= \partial_\theta u(t,2\pi) & t\geq 0, \end{cases} \tag{1.1}$$

where $m>0$ and $J*u(t,\theta)=K\int_0^{2\pi}\sin(\theta-\varphi)u(t,\varphi)d\varphi$, with u_0 even, $u_0(\cdot)\geq 0$ and $\int_{-\pi}^{\pi}u_0(\theta)d\theta=1$ and $K\geq 0$ is a constant. In the following we denote $x_1=x_1(u)=\int_0^{2\pi}u(\theta)\cos(\theta)d\theta$ for any $u\in L^1([0,2\pi])$. The right hand side of this equation is comprised of two components, with the first representing a nonlinear diffusion and the second one a nonlocal advection term. The dynamics of the solutions result from competition between these two terms, as the first one tends to spread solutions whereas the second one, on the contrary tends to concentrate them. In this work we examine the changes in the dynamics of the above equation depending on the parameters m and K, which control, respectively the diffusion and the strength of advection.

For the special case of linear diffusion, i.e. $m=1$, this equation arises in various contexts, including as a mean-field spin X-Y models [35], a Doi-Onsager or Smoluchowski model for nematic polymers [15, 16, 43], or a Kuramoto or Sakaguchi model of synchronization [1, 36, 20]. Its equilibria set and dynamics have been analyzed in great detail [28, 16, 35, 7, 20, 37, 17, 1] [15, 7, 43, 20]. The picture that emerges from these studies is that there are two distinct regimes depending on the value of K. On the one hand, for $K\leq\frac{1}{2}$, all solutions tend to the trivial equilibrium $u=1/(2\pi)$. On the other hand, for $K>\frac{1}{2}$, the equation admits a unique non trivial equilibrium (up to a rotation) that attracts all solutions except those that lie on the stable manifold of the trivial equilibrium. The non trivial equilibria are called *coherent* because they have a single maximum on $[-\pi,\pi]$, corresponding to a region of maximal density, where the population described by u aggregates. In this sense, the bifurcation taking place at $K=\frac{1}{2}$ separates a regime where diffusion dominates from the one where advection promotes coherence. This transition whereby the number of equilibria of the system changes as K crosses a critical value is

Date: February 28th, 2012.

the key property of the model. This sudden change of dynamics accounts for phenomena such as onset of synchrony in coupled oscillators, and the transition from isotropic to nematic phase in Doi-Onsager models. We refer to it as a coherence transition. Its characterization is one of the main motivations for the large number of studies devoted to this model. In the present work, our purpose is to analyze the impact of nonlinear diffusion (i.e. $m > 1$) on this transition.

Nonlinear diffusion equations, with or without advection, have been studied as mathematical models for many important phenomena, such as diffusions in porous media or spread of biological populations, that show original and complex dynamics [6, 24, 10, 19, 32, 22, 23, 25, 5, 18, 14]. In the context of biological aggregation, equations such as (1.1), with space variable $\theta \in \mathbb{R}^d$, $m > 1$ and various coupling functions, have been subject to an intense study, including mathematical results on derivation and well-posedness of the equation ([31, 27, 8, 9, 26, 30, 12]), and several phenomena that were known for the Porous Medium Equation (PME) [2, 3, 4, 42] such as finite propagation speed of interfaces and existence of travelling waves or stationary solutions [11, 41, 31, 29, 13]. Degenerate diffusion ($m > 1$) has been introduced as a biologically realistic mechanism for the apparition of clumps in aggregation models, i.e. the apparition of small groups of individuals with sharp edges, which had only been previously observed in one dimensional models with highly specific coupling kernels. In case $m = 2$ and for a general class of coupling functions J, Burger and al. [11] have studied the existence or non existence of equilibria in any dimension ($\theta \in \mathbb{R}^d$), and uniqueness, monotony and compact support properties of equilibria in dimension one ($\theta \in \mathbb{R}$). Taking $m = 3$ and $J(\theta) = Ke^{-|\theta|}$, and considering equation (1.1) with $\theta \in \mathbb{R}$, Topaz and al. [41] have shown in particular that depending on the coupling strength, various equilibria or periodic solutions with compact support exist. Degenerate diffusion has been introduced and considered in several other diffusion advection reaction equations. See [39, 38, 40] for the classical Keller-Segel model of chemotaxis with degenerate diffusion for example. Despite this large number of studies, to our knowledge, the effect of nonlinear diffusion $m > 1$ in equations of the form (1.1) has never been investigated so far. This is the aim for our paper.

Our main results are summarized in the following theorem:

Theorem 1.1. *For all $m \geq 1$ and $K > 0$, equation (1.1) is the gradient flow of a free energy and all smooth solutions converge to the set of equilibria of (1.1). Denoting $\tilde{K} = K\frac{1}{m}\left(\frac{1}{2\pi}\right)^{-(m-1)}$, except for $m = 2$ and $\tilde{K} = 2$ this set of equilibria is finite.*

For any $m \geq 1$ we have:

- *For all $\tilde{K} < 2$, the uncoherent equilibrium $\frac{1}{2\pi}$ is locally stable.*
- *For all $\tilde{K} > 2$, there is a unique pair of (locally stable) coherent equilibria of (1.1) whose bassins of attraction contain an open and dense set of initial conditions.*

When $1 \leq m \leq 2$, for all $\tilde{K} < 2$ the uncoherent equilibrium is globally stable.
When $m > 2$, there is a $0 < K_c(m) < 2$ such that

- *when $\tilde{K} < K_c$ the uncoherent equilibrium is globally stable,*
- *when $K_c < \tilde{K} < 2$ the dynamics of (1.1) is bistable: the uncoherent equilibrium $\frac{1}{2\pi}$ is locally stable, there is unique pair of (locally stable) coherent equilibria of (1.1), and all solutions of (1.1) converge to one of those.*

When $m = 1$, the coherent equilibria of (1.1) are positive on $[-\pi, \pi]$ for all $K > 0$. However, for all $m > 1$, there is a $K_l(m) \geq K_c(m)$ such that for all $\tilde{K} > K_l$, the coherent equilibria of (1.1) are localized in $[-\pi, \pi]$.

This theorem shows that nonlinear diffusion, besides localizing equilibria, modifies the scenario of transition to coherence. This modification is captured by the two-parameter bifurcation diagrams of equation (1.1) in the plane $(\tilde{K}, m)$ represented in fig. 1 (wherein the left panel is a magnification of a section of the right panel). These diagrams show that $(\tilde{K}, m) = (2, 2)$ where a highly degenerate pitchfork bifurcation takes place is an organizing center of the dynamics. Three qualitatively distinct

regimes labelled as (U), (B) and (C) come to meet at this point. These regimes represent, respectively, (i) the parameter range for which the uncoherent equilibrium $\frac{1}{2\pi}$ is globally asymptotically stable, (ii) the multistablity regime where $\frac{1}{2\pi}$ is locally stable and coexists with two pairs of coherent equilibria, with one pair being unstable and the other stable, and finally (iii) the regime of coherence where $\frac{1}{2\pi}$ is unstable and most solutions converge to either one of a pair of symmetrical stable coherent equilibria.

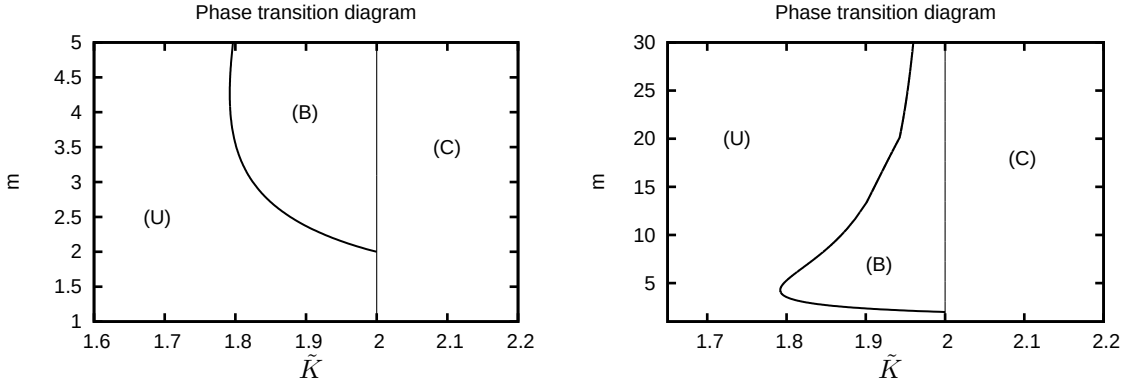

FIGURE 1. Equilibria bifurcation diagram. Solutions of (1.1) converge to the unique (uncoherent) equilibrium $\frac{1}{2\pi}$ in region (U). In region (C), solutions typically converge to the unique coherent equilibrium, with support strictly included in $[0, 2\pi]$ in region (C_l). In region (B) one coherent and one uncoherent (locally) stable equilibrium coexist. m and K are the parameters of (1.1), and $\tilde{K} = K\frac{1}{m}\left(\frac{1}{2\pi}\right)^{-(m-1)}$.

This paper is organized as follows. In section 2, we show that, as in the case $m = 1$ or in the PME case, equation (1.1) preserves positivity and L^1 mass. In section 3 we introduce the free energy of (1.1), which allows to write equation (1.1) as a gradient flow in the formalism of [34, 33]. A consequence is that all solutions of (1.1) converge to its equilibria set when $t \to +\infty$. We further show that at each equilibrium point the linearization of (1.1) is symmetric for an appropriately chosen scalar product. In section 4, we give existence and uniqueness results for equilibria of (1.1) and give analytical formula. This shows that the pitchfork bifurcation at $\frac{1}{2\pi}$ is supercritical when $1 < m < 2$ (section 5.1) and subcritical when $m > 2$ (section 5.2). When $m = 2$, the pitchfork bifurcation is infinitely degenerate, we have $\tilde{K} - 2 = o(x_1^n)$ for all $n \geq 2$ in a neighborhood of the bifurcation, where x_1 is the order parameter that characterizes equilibria in bifurcation diagrams, $x_1 = 0$ corresponding to the uncoherent equilibrium and $x_1 > 0$ to coherent equilibria. This bifurcation scenario and the transition from supercritical to subcritical pitchfork at $m = 2$ are shown in section 5.3. The bifurcation scenario in the limit $m \to +\infty$ is discussed in section 5.4. Several remarks and discussions are in section 6. Details on numerical methods used to make figures of this text can be found in the appendix.

2. Positivity and mass conservation

The problem (1.1) is reflexion invariant: if $u(t, \theta)$ is a solution of (1.1) then $v(t, \theta) = u(t, -\theta)$ is also a solution of (1.1) with $v_0(\theta) = u_0(-\theta)$. In particular, if u_0 is an even function then any solution $u(t, \cdot)$ of (1.1) is even. Here we focus only on even initial data and we suppose $u_0(\theta) = u_0(-\theta)$ in the following. If $u_0 \in L^1(\mathbb{S})$ with $u_0 \geq 0$, and $u(t, \cdot)$ is an associated solution of (1.1) on $[0, T]$, then we have $u(t, \cdot) \geq 0$ and $\int_{\mathbb{S}} u(t, \theta)d\theta = \int_{\mathbb{S}} u_0(\theta)d\theta$ for all $t \in [0, T]$ (see lemma 1). In the following we assume $u_0 \geq 0$ and

$\int_{\mathbb{S}^1} u_0(\theta)d\theta = 1$. We use the notation

$$u(t,\theta) = \frac{1}{2\pi} + \frac{1}{\pi}\sum_{n\geq 1} x_n(t)\cos(n\theta),$$

and in particular we denote $x_1 = x_1(u) = \int_0^{2\pi} u(\theta)\cos(\theta)d\theta$.

Lemma 1. *Assume that $u_0 \in L^1$ and u is a weak solution of (1.1) in $C^1([0,T], L^1([0,2\pi]))$. Then we have $\int_{-\pi}^{\pi} u(t,\theta)d\theta = \int_{-\pi}^{\pi} u_0(\theta)d\theta$ for all $t \in [0,T]$. Suppose that $u \in C^1([0,T], L^1([0,2\pi]))$ is a weak solution of (1.1) with $u(0,\cdot) = u_0 \geq 0$. Then we have $u(t,\cdot) \geq 0$ for all times $t \in [0,T]$.*

Proof. For any time $t \in [0,T]$ and $\phi \in C^\infty([0,T]\times[0,2\pi])$, we have

$$\int_0^{2\pi} u(t,\theta)\phi(\theta)d\theta = \int_0^{2\pi} u_0(\theta)\phi(\theta)d\theta + \int_0^T\int_0^{2\pi} \left(u(s,\theta)^m\partial_\theta^2\phi(s,\theta) - u(s,\theta)J*u(s,\theta)\partial_\theta\phi(s,\theta)\right)d\theta ds,$$

and for $\phi(s,\theta) = 1$ we find $\int_{-\pi}^{\pi} u(t,\theta)d\theta = \int_{-\pi}^{\pi} u_0(\theta)d\theta$ for all $t \leq T$.

Consider $u_-(t,\theta) = \max(-u(t,\theta),0) \geq 0$. We have $u_- \in C^1([0,T], L^1([0,2\pi]))$ and u_- is a weak solution of (1.1). Then the first part of the lemma gives $\int_0^{2\pi} u_-(t,\theta)d\theta = \int_0^{2\pi} u_-(0,\theta)d\theta = 0$ for all $t \in [0,T]$. With $u_- \geq 0$ this implies $u(t,\cdot) = 0$ and then $u(t,\cdot) \geq 0$ for all $t \in [0,T]$. □

3. Gradient Flows

3.1. **Energy decay and convergence to steady states.** In all this section, we assume $m > 1$. Equation (1.1) can be written as a gradient flow for the Wasserstein metric: taking

$$\mathcal{F}(u) = \frac{1}{m-1}\int_{\mathcal{S}} u^m(\theta)d\theta - \frac{K}{2}\iint_{\mathcal{S}\times\mathcal{S}} u(\theta)u(\varphi)\cos(\theta-\varphi)d\theta d\varphi, \tag{3.1}$$

we have formally

$$\frac{\delta\mathcal{F}}{\delta u} = \frac{m}{m-1}u^{m-1} - K\int_{\mathcal{S}}\cos(\theta-\varphi)u(\varphi)d\varphi, \tag{3.2}$$

and

$$\partial_\theta\left(u\partial_\theta\frac{\delta\mathcal{F}}{\delta u(\theta)}\right) = \partial_\theta\left(muu^{m-2}\partial_\theta u + Ku\int_{\mathcal{S}}\sin(\cdot-\varphi)u(\varphi)d\varphi\right), \tag{3.3}$$

so that (1.1) is equivalent to

$$\partial_t u = \partial_\theta\left(u\partial_\theta\frac{\delta\mathcal{F}}{\delta u(\theta)}\right). \tag{3.4}$$

The functional $\mathcal{F}$ is a strict Lyapunov functional for (1.1). More precisely, if $u(t,\cdot)$ is a smooth non-constant solution of (1.1), we have

$$\begin{aligned}\partial_t\mathcal{F}(u(t)) = D\mathcal{F}(u).\partial_t u &= \int_{\mathcal{S}}\frac{\delta\mathcal{F}}{\delta u(\theta)}.\partial_t u\, d\theta = -\int_{\mathcal{S}} u(t,\theta)\left[\partial_\theta\frac{\delta\mathcal{F}}{\delta u(\theta)}(t,\theta)\right]^2 d\theta \\ &= -\int_{\mathcal{S}} u\left(mu^{m-2}\partial_\theta u + Kx_1\sin(\cdot)\right)^2 d\theta < 0\end{aligned} \tag{3.5}$$

The solutions $\hat{u} \in L^\infty$ with $\partial_\theta(\hat{u}^{m-1}) \in L^\infty$ of

$$\hat{u}(\theta)\left(\frac{m}{m-1}\partial_\theta(\hat{u}^{m-1})(\theta) + K\hat{x}_1\sin(\theta)\right) = 0, \tag{3.6}$$

where $\hat{x}_1 = \int_{\mathcal{S}}\hat{u}(\theta)\cos(\theta)d\theta$, are the equilibria of equation (1.1) (see section 4 for a description of the set of solutions of (3.6)).

Proposition 3.1. *The functional $\mathcal{F} : L^m(\mathbb{S}) \to \mathbb{R}$ defined in (3.1) is C^1. If $u \in L^m(\mathbb{S})$ with $u \geq 0$ and $\int_{\mathbb{S}} u\, d\theta = 1$, then we have*

$$-\frac{K}{2} \leq \frac{m}{m-1}\|u\|_{L^m}^m - \frac{K}{2} \leq \mathcal{F}(u) \leq \frac{m}{m-1}\|u\|_{L^m}^m + \frac{K}{2} \tag{3.7}$$

Proof. The regularity of $\mathcal{F}$ is a direct consequence of its definition (3.1). The hypotheses $u \geq 0$ and $\int u d\theta = 1$ imply in particular $0 \leq x_1(u) \leq 1$, and the inequalities on $\mathcal{F}(u)$ follow. □

Theorem 3.2. *Assume that u is a solution of (1.1) with $u(t,\cdot) \geq 0$ and $\int_{\mathcal{S}} u(t,\theta)d\theta = 1$ for all $t \geq 0$, and $u \in C^1([0,+\infty[, L^m(\mathbb{S}))$. Let C be the set of solutions of (3.6).*

Then we have

$$dist_{L^\infty}(u(t), C) = \inf_{\hat{u}\in C} \|u(t) - \hat{u}\|_{L^\infty} \underset{t\to+\infty}{\longrightarrow} 0. \tag{3.8}$$

Remark. Lemma 1 and theorem 3.2 directly extend to initial data with $u_0 \geq 0$ and $\int_{-\pi}^{\pi} u_0(\theta)d\theta < +\infty$ only. In particular, solutions of (1.1) converge to its equilibria set even for non-even initial conditions. This also holds when $m = 1$, see [7].

Proof. For all $t \geq 0$ we have $\|u(t)\|_{L^m}^m \leq \mathcal{F}(u(t)) + \frac{K}{2} \leq \mathcal{F}(u(0)) + \frac{K}{2}$, and we have $u \in L^\infty([0,+\infty[, L^m)$ or equivalently $u^m \in L^\infty([0,+\infty[, L^1)$. By hypothesis and proposition 3.1, the function $t \mapsto \mathcal{F} \circ u(t)$ is $C^1([0,+\infty[, \mathbb{R})$, not increasing and bounded below. Hence we have $\mathcal{F}(u(t)) \to l \geq -\frac{K}{2}$ and $\partial_t \mathcal{F}(u(t)) \to 0$ when $t \to +\infty$.

Let $t_n \geq 0$ be a diverging sequence and $u_n = u(t_n, \cdot)$. The sequence (u_n) is bounded in L^m and (up to taking a subsequence), we can assume that $u_n \overset{wL^m}{\longrightarrow} u_\infty$ (where $\overset{wL^p}{\longrightarrow}$ denotes weak convergence in L^p space). We also have

$$\int_{\mathcal{S}} u_n \left(m u_n^{m-2}\partial_\theta u + K x_1(u_n)\sin(\cdot)\right)^2 d\theta \longrightarrow 0,$$

and $m u_n^{m-\frac{3}{2}}\partial_\theta u + K x_1(u_n)\sqrt{u_n}\sin(\cdot)$ is convergent in $L^2(\mathbb{S})$. We have $u_n \overset{wL^1}{\longrightarrow} u_\infty$, so that $x_1(u_n) \to x_1(u_\infty)$, and

$$K x_1(u_n)\sqrt{u_n}\sin(\cdot) \overset{wL^{2m}}{\longrightarrow} K x_1(u_\infty)\sqrt{u_\infty}\sin(\cdot).$$

In particular $m u_n^{m-3/2}\partial_\theta u_n = \frac{m}{m-\frac{1}{2}}\partial_\theta\left(u_n^{m-1/2}\right)$ is bounded in $L^{2m} \subset L^2$. Then $u_n^{m-1/2}$ is bounded in H^1 and compact in L^∞. Since $u_n^{m-1/2} \longrightarrow u_\infty^{m-1/2}$ weakly in $L^{\frac{m}{m-1/2}}$, we have $u_n^{m-1/2} \longrightarrow u_\infty^{m-1/2}$ in L^∞, and we deduce $u_n \longrightarrow u_\infty$ in L^∞. The limit $u_\infty \in L^\infty$ satisfies $\partial_\theta\left[u_\infty\left(\frac{m}{m-1}\partial_\theta u_\infty^{m-1} + K x_1 \sin(\theta)\right)\right] = 0$ at least in the sense of distributions. Since $\partial_\theta u_\infty^{m-1} \in L^\infty$, we have $u_\infty \in C$.

We have shown that the limit u_∞ of any converging subsequence $u(t_n, \cdot)$ is in the equilibria set C, and (3.8) follows. □

3.2. **Linearization at coherent equilibria.** Recall that we consider equation (1.1) in a functions space with $u \geq 0$, $\int_{\mathbb{S}} u\, d\theta = 1$ and u is even: $u(\theta) = u(-\theta)$. In this section, u denotes an equilibrium of equation (1.1).

Consider v, w such that $\int_{\mathbb{S}} v d\theta = \int_{\mathbb{S}} w d\theta = 0$. Suppose that they are V and W such that

$$v = \partial_\theta(u\partial_\theta V) \quad \text{and} \quad w = \partial_\theta(u\partial_\theta W). \tag{3.9}$$

Then we have (see [34, 33] for example)

$$\int_{\mathbb{S}} v W d\theta = \int_{\mathbb{S}} V w d\theta = -\int_{\mathbb{S}} u\partial_\theta V \partial_\theta W d\theta.$$

For such v and w, we define the bilinear form $(v,w) = -\int_{\mathbb{S}} v W d\theta = -\int_{\mathbb{S}} V w d\theta$ (note that $(\,,)$ depends on u). For such a $v \neq 0$ we have $(v,v) > 0$, and then $v, w \mapsto (v,w)$ defines a scalar product.

Proposition 3.3. *Let L_u be the operator associated to the linearization of (1.1) at the equilibrium u,*

$$L_u v = \partial_\theta \left(m u^{m-1} \partial_\theta v + v J * u + u J * v \right).$$

Let v, w be even and chosen as above. Then we have

$$(L_u v, w) = -m \int_{\mathbb{S}} u^{m-2}(\theta) v(\theta) w(\theta) d\theta + \int_{\mathbb{S}} \tilde{J} * v(\theta) w(\theta) d\theta = (v, L_u w), \tag{3.10}$$

where $\tilde{J}(\theta) = K \cos(\theta)$. In particular, the operator L_u is symmetric for the scalar product $(\,,)$.

Proof. We have

$$(L_u v, w) = \int_{\mathbb{S}} \left(m u^{m-1} \partial_\theta v + v J * u + u J * v \right) \partial_\theta W d\theta.$$

With $\partial_\theta(u^m) + u J * u = 0$, this gives

$$\begin{aligned} (L_u v, w) &= \int_{\mathbb{S}} \left(m u^{m-1} \partial_\theta \left(\frac{1}{u} v \right) + J * v \right) u \partial_\theta W d\theta \\ &= -m \int_{\mathbb{S}} u^{m-2} v w d\theta - m \int_{\mathbb{S}} \partial_\theta(u^{m-1}) v \partial_\theta W d\theta - \int_{\mathbb{S}} \tilde{J} * v w d\theta. \end{aligned} \tag{3.11}$$

Since u^{m-1}, v, and $\partial_\theta W$ are even, we have $\int_{\mathbb{S}} \partial_\theta(u^{m-1}) v \partial_\theta W d\theta = 0$ and the first equality of (3.10) follows. We have

$$\int \tilde{J} * v(\theta) w(\theta) d\theta = \iint K \cos(\theta - \varphi) v(\varphi) w(\theta) d\varphi d\theta,$$

hence the second term of (3.10) is symmetric in v and w, and we have $(L_u v, w) = (v, L_u w)$. □

The importance of the above result lies in that self-adjoint operators with compact resolvent have real pure point countable spectra, and they are diagonalizable in a Hilbert eigenbasis. The existence of spectral gap is then sufficent to show hyperbolicity and linear stability of equilibria, and classical stable, central and unstable manifolds existence theorem are available. This allows for the definition of an approriate projections and the study of small perturbations effects on the dynamics in neighborhoods of the equilibria set (see [7, 20, 21] in case $m = 1$).

4. Structure of the set of equilibria

To serve as a basis for comparison, we recall briefly the bifurcation scenario in case $m = 1$ (see [28, 16, 35, 7, 20]). When the coupling strength is below a critical value K_c, equation (1.1) has a unique (stable) equilibrium $\frac{1}{2\pi}$ that is called uncoherent. When $K = K_c$ a supercritical pitchfork bifurcation occurs, and for all $K > K_c$ there are exactly three equilibria: $\frac{1}{2\pi}$ and $u(\theta) = \frac{1}{c} e^{\alpha \cos(\theta)}$, where $c = \int_{-\pi}^{\pi} e^{\alpha \cos(\theta)} d\theta$ and $\alpha = \int_{-\pi}^{\pi} u(\theta) \cos(\theta) d\theta$, and $u(\cdot + \pi)$. When $K > K_c$, this equilibrium u is locally stable and attracts all solutions of (1.1) such that $\int_{-\pi}^{\pi} u_0(\theta) \cos(\theta) d\theta > 0$, whereas all solutions with $\int_{-\pi}^{\pi} u_0(\theta) \cos(\theta) d\theta < 0$ converge to $u(\cdot + \pi)$. These two equilibria are non constant, they have a unique maximum on $[-\pi, \pi]$ and they are called coherent in that sense. In particular, coherent equilibria have been shown to diverge from $\frac{1}{2\pi}$ as $(K - K_c)^{\frac{1}{2}}$ ([1, 37, 17] and references therein).

In this section, we establish the main elements of proof of theorem 1.1. In the next section 5 we detail further bifurcations scenario (depending on m), which lead to the phase transition diagram of figure 1.

4.1. The uncoherent equilibrium $\frac{1}{2\pi}$.

A pitchfork bifurcation occurs at the uncoherent equilibrium when $K = K_b = 2m \left(\frac{1}{2\pi} \right)^{m-1}$. The uncoherent equilibrium is linearly stable when $K < K_b$ and unstable when $K > K_b$. In the following we rescale the parameter $\tilde{K} = K \frac{1}{m} \left(\frac{1}{2\pi} \right)^{-(m-1)}$, so that the bifurcation occurs at $\tilde{K} = 2$ independently of m.

Proposition 4.1. *For all $m > 0$ and $K \geq 0$, $u(\theta) = \frac{1}{2\pi}$ is an equilibrium of equation (1.1). The linearization of equation (1.1) at $\frac{1}{2\pi}$ is:*

$$\partial_t v = L_{\frac{1}{2\pi}} v = m \left(\frac{1}{2\pi}\right)^{m-1} \partial_\theta^2 v + \frac{K}{2\pi} x_1 \cos(\theta), \tag{4.1}$$

the operator $L_{\frac{1}{2\pi}}$ is orthogonal is the classical Fourier basis of $L^2(\mathbb{S})$ and its spectrum is given by $\lambda_1 = \frac{K}{2} - 2m\left(\frac{1}{2\pi}\right)^{m-1}$ and $\lambda_n = -n^2 2m\left(\frac{1}{2\pi}\right)^{m-1}$ for all $n \geq 2$.

In particular, $\frac{1}{2\pi}$ is linearly stable if and only if

$$K < K_b = 2m \left(\frac{1}{2\pi}\right)^{m-1}. \tag{4.2}$$

For $K = K_b$ the operator $L_{\frac{1}{2\pi}}$ has a null eigenvalue, and for $K > K_b$ the equilibrium $\frac{1}{2\pi}$ is linearly unstable.

4.2. **Coherent equilibria of equation (1.1).**

Proposition 4.2. *Suppose $m > 1$. Equilibria $\hat{u}$ of equation (1.1) satisfy either $\hat{u}(\theta) = \frac{1}{2\pi}$ or*

$$\hat{u}^{m-1} = \frac{m-1}{m} K x_1 \left[\cos(\theta) + c\right]_+, \tag{4.3}$$

with $\int_{-\pi}^{\pi} \hat{u}(\theta) d\theta = 1$ and $\int_{-\pi}^{\pi} \hat{u}(\theta)\cos(\theta) d\theta = x_1$ and $c > -1$, where x_+ denotes $\max(x, 0)$.

For every $c > -1$, there is a unique $K > 0$ and $x_1 \in]0, 1]$ such that (4.3) holds, they are given by

$$K = \frac{m}{m-1} \frac{1}{J_m(c)} \frac{1}{I_m(c)^{m-2}} \quad \text{and} \quad x_1 = \frac{J_m(c)}{I_m(c)}, \tag{4.4}$$

where $I_m(c) = \int_{-\pi}^{\pi} \left[\cos(\theta) + c\right]_+^{\frac{1}{m-1}} d\theta$ and $J_m(c) = \int_{-\pi}^{\pi} \left[\cos(\theta) + c\right]_+^{\frac{1}{m-1}} \cos(\theta) d\theta$.

In case $0 < m < 1$, the non-constant equilibria of equation (1.1) are

$$\hat{u}^{m-1} = \frac{1-m}{m} K x_1 \left[c - \cos(\theta)\right]_+, \tag{4.5}$$

with $c > 1$, where x_1 and K are given by

$$x_1 = \frac{\mathcal{J}_m(c)}{\mathcal{I}_m(c)} \quad \text{and} \quad K = \frac{m}{1-m} \frac{1}{\mathcal{J}_m(c)} \mathcal{I}_m(c)^{2-m}$$

with $\mathcal{I}_m(c) = \int_{-\pi}^{\pi} \left[c - \cos(\theta)\right]_+^{\frac{-1}{1-m}} d\theta$ and $\mathcal{J}_m(c) = \int_{-\pi}^{\pi} \left[c - \cos(\theta)\right]_+^{\frac{-1}{1-m}} \cos(\theta) d\theta$.

Proof. Assume that $m > 1$ and u is a non-constant equilibrium of (1.1). Following equation (3.6), for all $\alpha \in [0, 2\pi]$ we have either $u(\alpha) = 0$ or $u^{m-1}(\theta) = \frac{K(m-1)}{m} x_1 \left(\cos(\theta) + c\right)$ on an open interval containing α. With $u^{m-1} \in W^{1,\infty}(\mathbb{S})$ and $u \geq 0$, this implies $u^{m-1}(\theta) = \frac{K(m-1)}{m} x_1 \left(\cos(\theta) + c\right)_+$ on $[-\arccos(-c), \arccos(-c)]$, that is an increasing function of θ. Thus there is a unique c such that (4.3) holds on $\mathrm{Supp}(u) = [-\arccos(-c), \arccos(-c)]$ and $u^{m-1}(\theta) = 0$ on $[0, 2\pi] \backslash \mathrm{Supp}(u)$.

We have

$$\int_{-\pi}^{\pi} u(\theta) d\theta = \left(\frac{K(m-1)}{m} x_1\right)^{\frac{1}{m-1}} I_m(c) = 1, \tag{4.6}$$

$$\int_{-\pi}^{\pi} u(\theta)\cos(\theta) d\theta = \left(\frac{K(m-1)}{m} x_1\right)^{\frac{1}{m-1}} J_m(c) = x_1, \tag{4.7}$$

which give directly $x_1 = \frac{J_m}{I_m}$. Then we have $K\frac{m-1}{m} J_m(c)^{m-1} = x_1^{m-2}$ and (4.4) follows.

In case $0 < m < 1$, equation (4.5) is proved similarly. □

Proposition 4.4 shows in particular that the branch of equilibria of proposition 4.2 appears by a pitchfork bifurcation at $\frac{1}{2\pi}$ when $K = K_b$, or equivalently $\tilde{K} = 2$, and that it persists until $K \to +\infty$. Equation (4.12) shows that when $1 < m < 2$ the pitchfork bifurcation is supercritical, and when $m > 2$ the pitchfork bifurcation is subcritical. In both cases $1 < m < 2$ and $m > 2$, the distance between coherent equilibria and the uncoherent equilibrium scales as $\left(\tilde{K} - 2\right)^{1/2}$ in a neighborhood of the bifurcation. When $m = 2$ the pitchfork bifurcation degenerates, the distance between coherent equilibria and the uncoherent equilibrium is larger than some positive constant for any $\tilde{K} > 2$ (see also proposition 4.3 for the case $m = 2$).

Proposition 4.3. *In the case $m = 2$, (equations (4.4) still hold) the equilibria are given by*

- *for $c \geq 1$,*
$$K = \frac{2}{\pi} \quad \textit{and} \quad x_1 = \frac{1}{2c},$$
- *for $-1 < c < 1$,*
$$K = \frac{2}{\arccos(-c)} \quad \textit{and} \quad x_1 = \frac{\arccos(-c)}{2c\arccos(-c) + 2\sqrt{1-c^2}}.$$

Proof. In case $m = 2$, their respective definitions give $I_2(c) = 2c\arccos(-c) + 2\sqrt{1-c^2}$ for $|c| < 1$ and $I_2(c) = \frac{1}{2c}$ for $c \geq 1$, and $J_2(c) = \arccos(-c)$ for $|c| < 1$ and $J_2(c) = \pi$ for all $c \geq 1$. When $m = 2$ equation (4.7) reads $2K = J_m(c)$, and combined with $x_1 = \frac{J_m}{I_m}$, this implies property 4.3. □

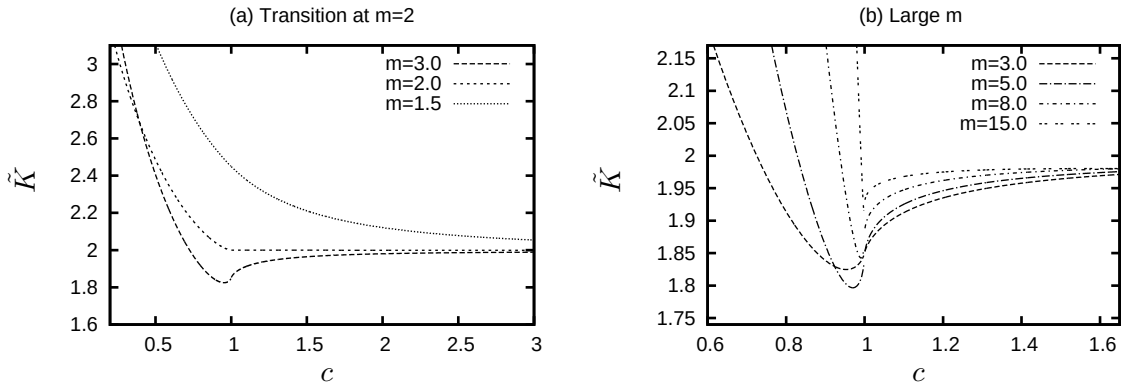

FIGURE 2. $\tilde{K}$ as a function of c for $m > 1$. Coherent equilibria of (1.1) are uniquely determined by $\tilde{K}$ and x_1, which depend on the parameter $c \in]-1;+\infty[$. When $1 < m < 2$, $\tilde{K}_m(c)$ is decreasing on $]-1;+\infty[$, and for every $\tilde{K} \in [2;+\infty[$, there is exactly one coherent equilibrium of (1.1). This is illustrated by the top most curve on the panel (a) for $m = 1.5$. For $m > 2$, $\tilde{K}_m(c)$ has a minimum at some $c^* < 1$, it is decreasing on $]-1, c^*]$ and increasing on $[c^*;+\infty[$. The below most curve on panel (a) and the the four curves on panel (b) show that this holds for various values of $K = 3.0$, $K = 5.0$, $K = 8.0$, and $K = 15.0$. For all m, we have $\tilde{K} \to 2$ when $c \to +\infty$. When $m > 2$, for all $\tilde{K} \in [\tilde{K}_m(c^*); 2]$ equation (1.1) has two coherent equilibria. They appear by a fold bifurcation when $\tilde{K} = \tilde{K}_m(c^*)$, and the unstable one disappears by subcritical pitchfork bifurcation at $\frac{1}{2\pi}$ when $\tilde{K} = 2$ (see proposition 4.2 and illustrations in figure 2)

Proposition 4.4. *Assume that $m > 1$.*

- *We have $|x_1| \leq 1$ and $K > 0$ for all $c \in]-1;+\infty[$.*

- *We have* $x_1 = 1 - \beta_m(1+c) + o(1+c)$ *and*
$$K = \frac{m}{m-1}\gamma_m^{1-m}(1+c)^{-\frac{m+1}{2}} + o(1+c)^{-\frac{m+1}{2}}, \tag{4.8}$$
when $c \to -1$*, where the constants* $\beta_m > 0$ *and* $\gamma_m > 0$ *are given in (4.16). In particular we have*
$$x_1 = 1 - \mu K^{-\frac{2}{m+1}} + o\left(K^{-\frac{2}{m+1}}\right) \quad \text{when} \quad K \to +\infty, \tag{4.9}$$
with $\mu = \beta_m \left(\frac{m-1}{m}\right)^{-\frac{2}{m+1}} \gamma_m^{-2\frac{m-1}{m+1}} > 0$.
- *When* $c \to +\infty$*, we have*
$$x_1 = \frac{1}{2(m-1)}\frac{1}{c}\left[1 + \frac{(2-m)(1-2m)}{8(m-1)^2}\frac{1}{c^2} + o\left(\frac{1}{c^2}\right)\right], \tag{4.10}$$
$$K = 2m\,(2\pi)^{1-m}\left[1 - \frac{2-m}{8(m-1)^2}\frac{1}{c^2} + o\left(\frac{1}{c^2}\right)\right], \tag{4.11}$$
and in particular
$$\tilde{K} - 2 = -(m-2)x_1^2 + o\left(x_1^2\right). \tag{4.12}$$

Proof. We have $I_m(c) > 0$ for all $c > -1$, and since $\theta \to (c + \cos(\theta))_+$ is not increasing and non negative on $[0, \pi]$, we have $J_m(c) \geq 0$. Furthermore we have $|J_m(c)| \leq I_m(c)$ for all $c > -1$, and the inequalities $|x_1| \leq 1$ and $K > 0$ follow.

Denoting $\epsilon = 1 + c$, we have
$$\begin{aligned} I_m(c) &= 2\int_0^{\arccos(-c)} (c + \cos(\theta))^{\frac{1}{m-1}}\, d\theta = 2\int_{-c}^{1} (c+y)^{\frac{1}{m-1}}\, \frac{1}{\sqrt{1-y^2}} dy \\ &= 2\sqrt{\epsilon}\,\epsilon^{\frac{1}{m-1}} \int_0^1 (1-\lambda)^{\frac{1}{m-1}}\, \frac{1}{\sqrt{\lambda(2-\epsilon\lambda)}} d\lambda, \end{aligned} \tag{4.13}$$
and similarly
$$J_m(c) = 2\sqrt{\epsilon}\,\epsilon^{\frac{1}{m-1}} \int_0^1 (1-\lambda)^{\frac{1}{m-1}}\, \frac{1-\epsilon\lambda}{\sqrt{\lambda(2-\epsilon\lambda)}} d\lambda. \tag{4.14}$$
This implies $x_1 \to 1$ in (4.8), and with $K = \frac{m}{m-1}\frac{1}{x_1}\frac{1}{(I_m)^{m-1}}$ we also have $K \to +\infty$ when $c \to -1$. More precisely, we have
$$x_1 = 1 - \beta_m\epsilon + o(\epsilon) \quad \text{and} \quad K = \frac{m}{m-1}\gamma_m^{1-m}\epsilon^{-\frac{m+1}{2}}\left(1 - \beta_m\epsilon + o(\epsilon)\right), \tag{4.15}$$
where
$$\gamma_m = 2\int_0^1 (1-\lambda)^{\frac{1}{m-1}} \frac{1}{\sqrt{\lambda(2-\lambda)}} d\lambda \quad \text{and} \quad \beta = \frac{2}{\gamma}\int_0^1 (1-\lambda)^{\frac{1}{m-1}} \frac{\lambda}{\sqrt{\lambda(2-\lambda)}} d\lambda, \tag{4.16}$$
and this implies (4.8) and (4.9).

Using the Taylor expansion $(1+x)^\alpha = 1 + \alpha x + \frac{\alpha(\alpha-1)}{2}x^2 + \frac{\alpha(\alpha-1)(\alpha-2)}{6}x^3 + O(x^4)$, we find
$$I_m(c) = c^{\frac{1}{m-1}} \int_{-\pi}^{\pi} \left(1 + \frac{1}{c}\cos(\theta)\right)^{\frac{1}{m-1}} d\theta = 2\pi c^{\frac{1}{m-1}} \left[1 + \frac{2-m}{4(m-1)^2}\frac{1}{c^2} + O\left(\frac{1}{c^4}\right)\right]. \tag{4.17}$$
when $c \to +\infty$. Similarly, we have
$$J_m(c) = \pi c^{\frac{1}{m-1}} \frac{1}{m-1}\frac{1}{c}\left(1 + \frac{(3-2m)(2-m)}{8(m-1)^2}\frac{1}{c^2} + O\left(\frac{1}{c^4}\right)\right). \tag{4.18}$$
The estimate (4.10) on x_1 is a consequence of (4.4) and the two estimates above. The asymptotic of K is a consequence of this estimate on x_1 and $K = \frac{m}{m-1}\frac{1}{x_1}\frac{1}{(I_m(c))^{m-1}}$. Equation (4.12) is a consequence of (4.10) and (4.11) □

The bifurcations in cases $1 < m < 2$, $m = 2$, $m > 2$ and the transition at $m = 2$ are discussed in the following sections. The case $m \to +\infty$ is also discussed in section 5.4.

5. Global description of results

After this analysis of the equilibria set of equation (1.1), we synthesize our findings by presenting, for various ranges of the nonlinear diffusion coefficient m, the corresponding bifurcation diagrams when the parameter $\tilde{K}$ is varied. One of the main ingredients in our analysis of equilibria and their dependence on parameters has been the function $c \to \tilde{K}$. It is the shape of this function that determines the number of non trivial equilibria of the system. The left panel in figure 2 illustrates how this function changes for various values of the parameter m. For $1 < m < 2$, it is strictly decreasing while for $m > 2$ it exhibits a unique minimum. In between, at $m = 2$, the function is strictly decreasing with a zero slope at its right hand limit. The right panel of the same figure shows how the general shape and the minimal value of the function change when m is further increased. In the following paragraphs, we describe the dynamics of the system for these three cases of m and illustrate through numerical computations of representative examples how this change in the shape of $c \to \tilde{K}$ translates into the properties of equation (1.1).

5.1. **Coherence transition for $1 < m < 2$.** When $1 < m < 2$ the function $\tilde{K} = \tilde{K}(c)$ is decreasing on $]-1, +\infty[$ (see illustration figure 2 panel (a) for $K = 1.5$), and the function $x_1 = x_1(c)$ is decreasing on $]-1, +\infty[$. The bifurcation diagram $x_1 = x_1(\tilde{K})$ is shown in figure 3 panel (a).

When $\tilde{K} < \tilde{K}_c = 2$ the unique equilibrium of (1.1) is the uncoherent steady state $\frac{1}{2\pi}$ (corresponding to $x_1 = 0$), which is locally and globally stable (label (P_1) figure 3 panel (a)). At $\tilde{K} = \tilde{K}_c = 2$ a supercritical pitchfork bifurcation occurs (see proposition 4.4). When $\tilde{K} > 2$, the uncoherent steady state $\frac{1}{2\pi}$ is locally unstable (label (P_2) figure 3 panel (a)) and equation (1.1) has a coherent equilibrium with $x_1 > 0$. When $\tilde{K} < \tilde{K}(c = 1) \approx 2.4$ this coherent equilibrium is positive on $[-\pi, \pi]$ (label (S_p) figure 3 panel (a)), whereas when $\tilde{K} > \tilde{K}(c = 1)$ this coherent equilibrium is localized: its support is strictly included in $]-\pi, \pi[$ (label (S_l) figure 3 panel (a)).

When $1 < m < 2$, solutions $u(t, \theta)$ of (1.1) are smooth for all times $t \geq 0$. When $\tilde{K} < \tilde{K}_c$, all solutions converge to the uncoherent equilibrium $\frac{1}{2\pi}$. Figure 4 panels (d) and (e) show one such converging solution for $\tilde{K} = 1.5$.

When $\tilde{K} > \tilde{K}(c = 1)$ most solutions converge to the coherent equilibrium (S_l) of (1.1) with localized support (see illustration in figure 4 panel (f) for $\tilde{K} = 6.0$).

5.2. **Coherence transition when $m > 2$.** When $m > 2$ the function $x_1 = x_1(c)$ is decreasing on $]-1, +\infty[$, and the function $\tilde{K} = \tilde{K}(c)$ is decreasing on $]-1, c^*[$, it has a unique minimum at $c = c^* < 1$ and it is increasing on $]c^*, +\infty[$ (in figure 2 see the lowest curve in panel (a) for $m = 3$, and panel (b) for $m = 3$, $m = 5$, $m = 8$, and $m = 15$). The value $\min_{c\in]-1,1[} \tilde{K}_m(c)$, that depends on m, defines the border of regions (U) and (B) in figure 1: at this value a fold bifurcation gives birth to two (localized) coherent equilibria. The equilibria given by (4.6) with $c < c^*$ are coherent, localized and (locally) stable. The equilibria given (4.6) with $c < c^*$ are coherent and unstable, for $c < 1$ they are localized and for $c > 1$ they are positive on $\mathbb{S}$.

When $\tilde{K} < \min_{c\in]-1,1[} \tilde{K}_m(c)$ the unique equilibrium of (1.1) is the uncoherent steady state $\frac{1}{2\pi}$, which is locally and globally stable (label (P_1) figure 5 panel (a)). When $\min_{c\in]-1,1[} \tilde{K}_m(c) < \tilde{K} < 2$, there is one coherent localized stable equilibrium denoted by label (S_l) in figure 5 panel (a), and illustrated for $\tilde{K} = 1.84$ by the lowest curve in figure 5 panel (d). For the same values $\min_{c\in]-1,1[} \tilde{K}_m(c) < \tilde{K} < 2$ there is also and one coherent unstable equilibrium that is localized for $\min_{c\in]-1,1[} \tilde{K}_m(c) < \tilde{K} < \tilde{K}(c = 1)$ (label (U_l) in panel figure 5 (a)), and positive for $\tilde{K}(c = 1) < \tilde{K} < 2$. (label (U_p) in figure 5 panel (a)). Panel

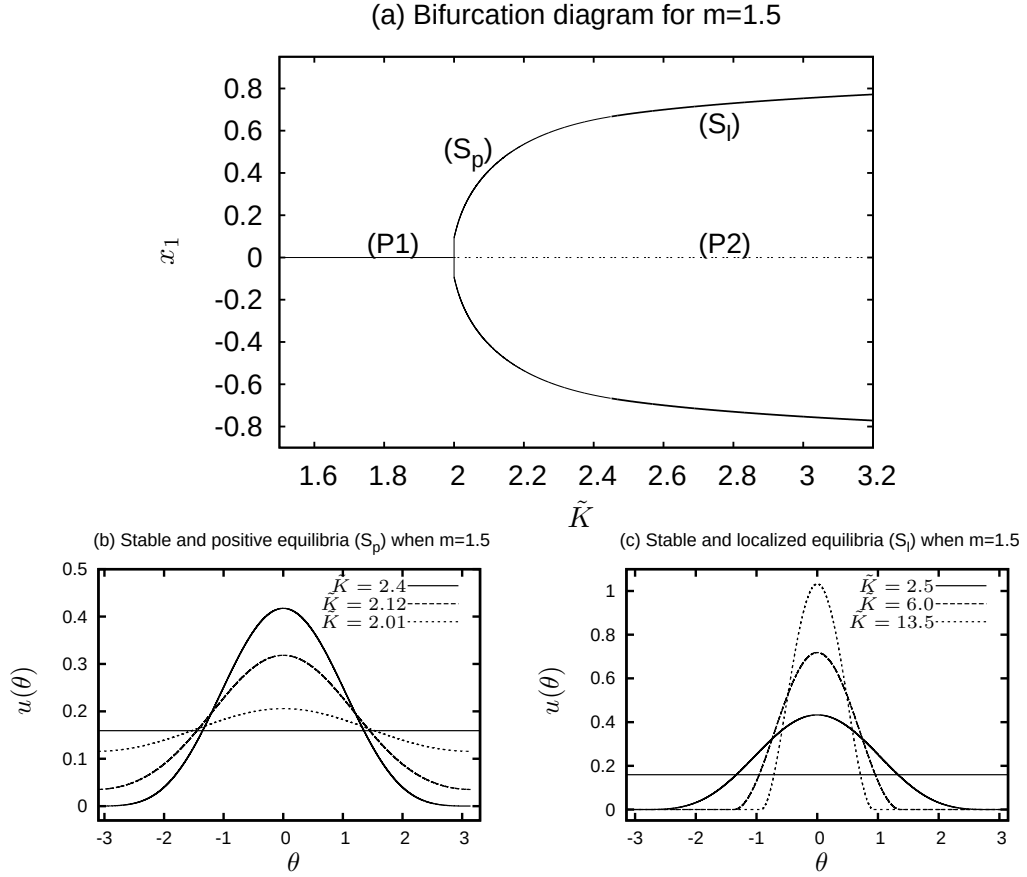

FIGURE 3. Equilibria bifurcation diagram and equilibria of (1.1) in case $m = 1.5$. Panel (a) show the number of equilibria of (1.1) for $0 < \tilde{K} < +\infty$. We see in particular the supercritical pitchfork bifurcation occurring at $\frac{1}{2\pi}$ when $\tilde{K} = 2$. The branch of stable equilibria that appear satisfies $\tilde{K} - \tilde{K}_c \sim -(m-2)x_1^2 > 0$ in a neighborhood of the bifurcation (see proposition 4.4). In panels (b) and (c) the horizontal line represents $\frac{1}{2\pi}$. Panel (b) shows the shape of coherent (stable) equilibria (S_p), for various values of $\tilde{K}$ in $]2, \tilde{K}(c=1)[$. These equilibria emerge from $\frac{1}{2\pi}$ when $\tilde{K} = 2$ and they remains positive until $\tilde{K} = \tilde{K}(c=1)$. Panel (c) shows the shape of localized coherent equilibria (S_l), for various values of $\tilde{K} > \tilde{K}(c=1)$. When $\tilde{K} = \tilde{K}(c=1)$ the equilibrium is non negative and zero exactly at $\theta = \pi$, and the equilibria are localized when $\tilde{K} > \tilde{K}(c=1)$. They converge to a Dirac mass centered at $\theta = 0$ when $K \to +\infty$. (see proposition (4.2) for analytical formulas for these equilibria). (Details on numerical methods used here can be found in the appendix.)

(c) in figure 5 shows the shape of such localized equilibrium when $\tilde{K} = 1.84$, and positive equilibria are shown for various $\tilde{K}(c=1)\tilde{K} < 2$ in panel (b). At $\tilde{K} = \tilde{K}_c = 2$ a subcritical pitchfork bifurcation occurs (see proposition 4.4). When $\tilde{K} > 2$, the uncoherent steady state $\frac{1}{2\pi}$ is locally unstable (label (P_2) figure 5 panel (a)) and equation (1.1) has a unique localized coherent equilibrium with $x_1 > 0$ (label (S_l) in figure 5 panel (a)). Two such equilibria are shown in figure 5 panel (d) for $\tilde{K} = 2.4$ and $\tilde{K} = 4.7$, and in panel (e) for $\tilde{K} = 7$, $\tilde{K} = 17$, $\tilde{K} = 100$ and $\tilde{K} = 400$.

When $\tilde{K} < \tilde{K}(c^*)$, all solutions converge to the uncoherent equilibrium $\frac{1}{2\pi}$ (region (U) in figure 1, label (P_1) in figure 5 panel (a)). In the multistability region (B) (see figure 1), corresponding to $\tilde{K}(c^*) < \tilde{K} < 2$, solutions typically converge either to the uncoherent equilibrium (P_1) or to a coherent

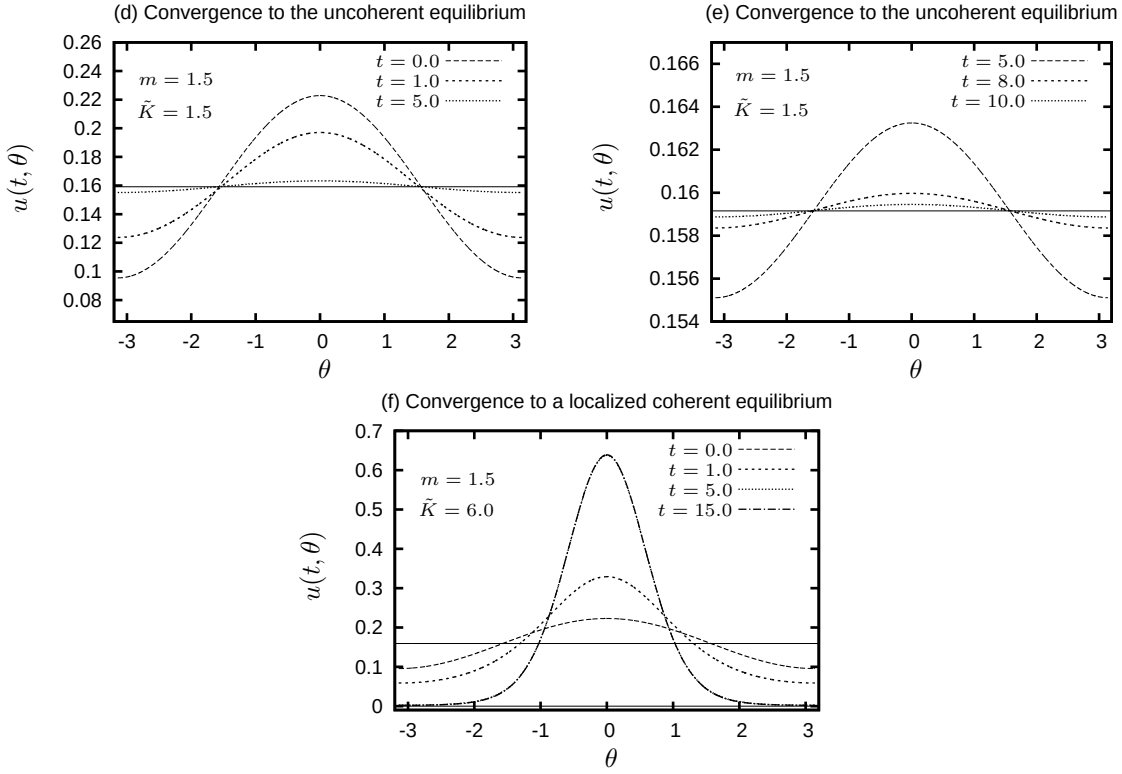

FIGURE 4. Convergence of solutions in case $m = 1.5$. When $\tilde{K} < 2$, solutions converge to the uncoherent equilibrium (P_1). This is illustrated in panels (d) and (e) where we used for initial condition $u_0 = \frac{1}{2\pi} + \frac{x_1(0)}{\pi}\cos(\cdot)$ with $x_1(0) = 0.2$, and we have $|x_1(t)| < 10^{-3}$ for all $t \geq 10.0$. Panel (f) illustrates convergence to the localized coherent equilibria (S_l) for $\tilde{K} > \tilde{K}(c = 1)$. We used $\tilde{K} = 6.0$, the solution remains smooth and positive before converging, and using the same initial condition that in panel (d) it has numerically converged for $t \geq 5$. (Details on numerical methods used here can be found in the appendix.)

localized equilibrium (S_l). This is illustrated in figure 6 panels (f) and (g). For the same value of $\tilde{K} = 1.86$ and two different initial conditions, we observe convergence to a coherent equilibrium in panel (f) and convergence to the uncoherent equilibrium in panel (g). When $\tilde{K} > 2$ (region (C) in figure 1), most solutions converge to the localized and coherent equilibrium (label (S_l) in panel (a) of figure 5). Panel (h) of figure 6 shows such a solution for $\tilde{K} = 7$.

5.3. **Coherence transition when** $m = 2$**.** When $m = 2$ the function $\tilde{K} = \tilde{K}(c)$ is decreasing on $]-1, 1[$ and constant on $[1, +\infty[$ (proposition 4.3, see illustations in figure 2 panel (a)), and the function $x_1 = x_1(c)$ is decreasing on $]-1, +\infty[$. The bifurcation diagram $x_1 = x_1(\tilde{K})$ is shown in figure 7 panel (a).

When $\tilde{K} < \tilde{K}_c = 2$ the unique equilibrium of (1.1) is the uncoherent steady state $\frac{1}{2\pi}$ (corresponding to $x_1 = 0$), which is locally and globally stable (label (P_1) figure 7 panel (a)). At $\tilde{K} = \tilde{K}_c = 2$ a degenerate pitchfork bifurcation occurs (proposition 4.3). Any u given by $u(\cdot) = \frac{1}{2\pi} + \frac{1}{\pi}x_1\cos(\cdot)$ with $0 \leq x_1 \leq \frac{1}{2}$ is an equilibrium of (1.1) (label (N_p) figure 3 panel (a)). The uncoherent equilibrium is recovered when $x_1 = 0$, for any $0 < x_1 < 0.5$ the equilibrium is positive on $[-\pi, \pi]$, and for $x_1 = 0.5$ the equilibrium is non negative on $[-\pi, \pi]$. When $m = 2$ the transition from uncoherence to coherence is sharp. The family of equilibria connecting $\frac{1}{2\pi}$ to the localized coherent equilibria appear all-at-once when $\tilde{K} = 2$. In particular we have $\tilde{K} - \tilde{K}_c = o(x_1^n)$ for any $n \geq 2$ in some neighborhood of the

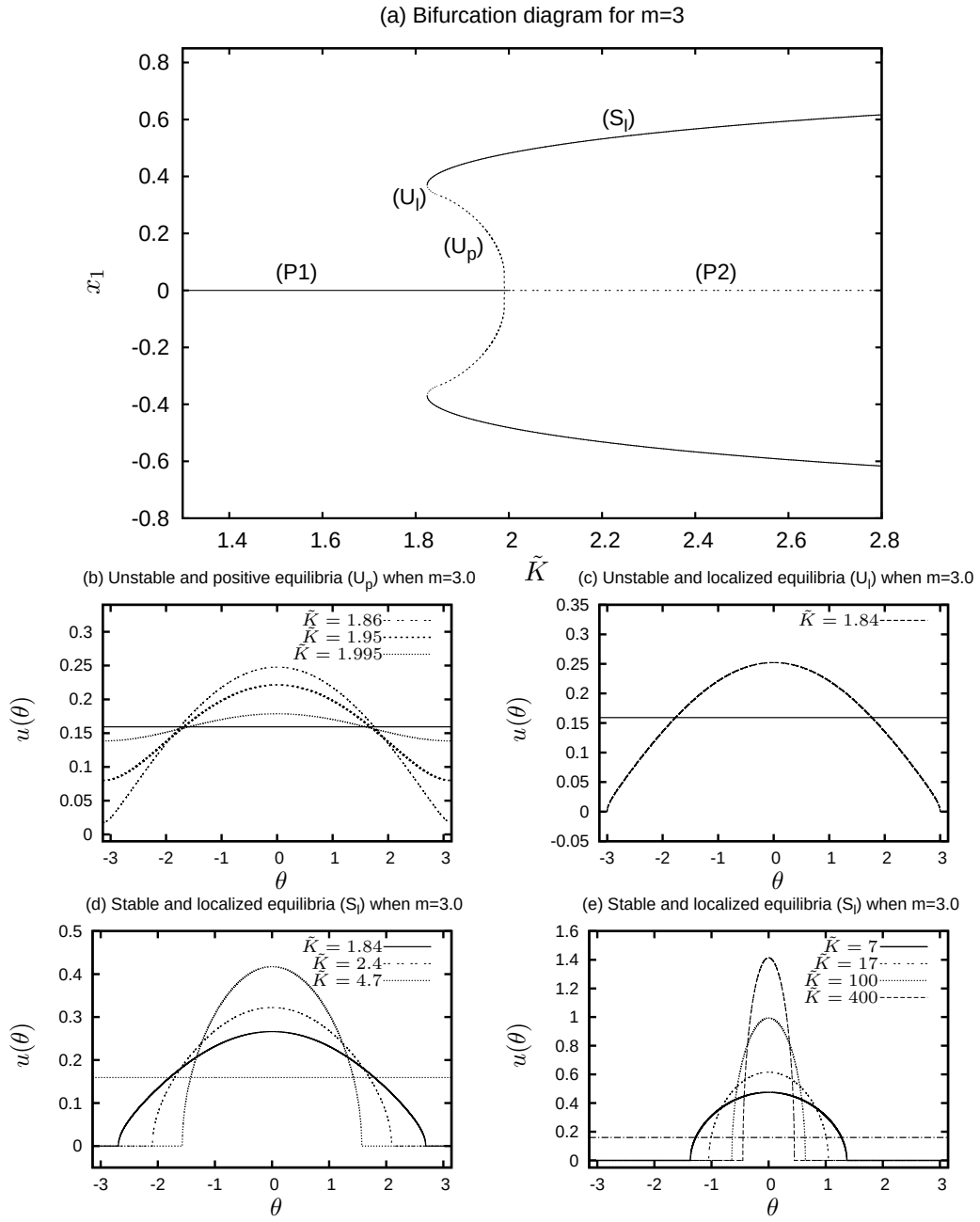

FIGURE 5. Equilibria bifurcation diagram, case $m = 3$. Panel (a) shows the number of equilibria of (1.1) for $0 < \tilde{K} < +\infty$. We see in particular the subcritical pitchfork bifurcation occurring at $\frac{1}{2\pi}$ when $\tilde{K} = 2$. The branch of unstable equilibria that disappear satisfies $\tilde{K} - \tilde{K}_c \sim -(m-2)x_1^2 > 0$ in a neighborhood of the bifurcation (see proposition 4.4). In panels (b) to (e), the horizontal line represents $\frac{1}{2\pi}$. Panel (b) shows the shape of unstable coherent equilibria (U_p), for various values of $\tilde{K}$ in $]\tilde{K}(c=1), 2[$. These equilibria are non negative when $\tilde{K} = \tilde{K}(c=1)$, and positive when $]\tilde{K}(c=1), 2[$. They converge to $\frac{1}{2\pi}$ when $\tilde{K} \to 2$. The shape of localized and unstable coherent equilibria (U_l), that exist for $\tilde{K}$ in $]\min \tilde{K}_m(c), \tilde{K}(c=1)[$ is illustrated in panel (c) for $\tilde{K} = 1.84$. These equilibria appear by fold bifurcation at $\tilde{K} = \min \tilde{K}_m(c)$, and they become positive when $\tilde{K} > \tilde{K}(c=1)$. Panels (d) and (e) show localized coherent (locally) stable equilibria (S_l), for various values of $\tilde{K} > \min \tilde{K}_m(c)$ (see proposition (4.2) for analytical formulas for coherent equilibria). These equilibria appear at $\tilde{K} = \min \tilde{K}_m(c)$ by fold bifurcation, they are localized and stable for all $\tilde{K} > \min \tilde{K}_m(c)$, and they converge to a Dirac mass at $\theta = 0$ when $\tilde{K} \to +\infty$. (Details on numerical methods used here can be found in the appendix.)

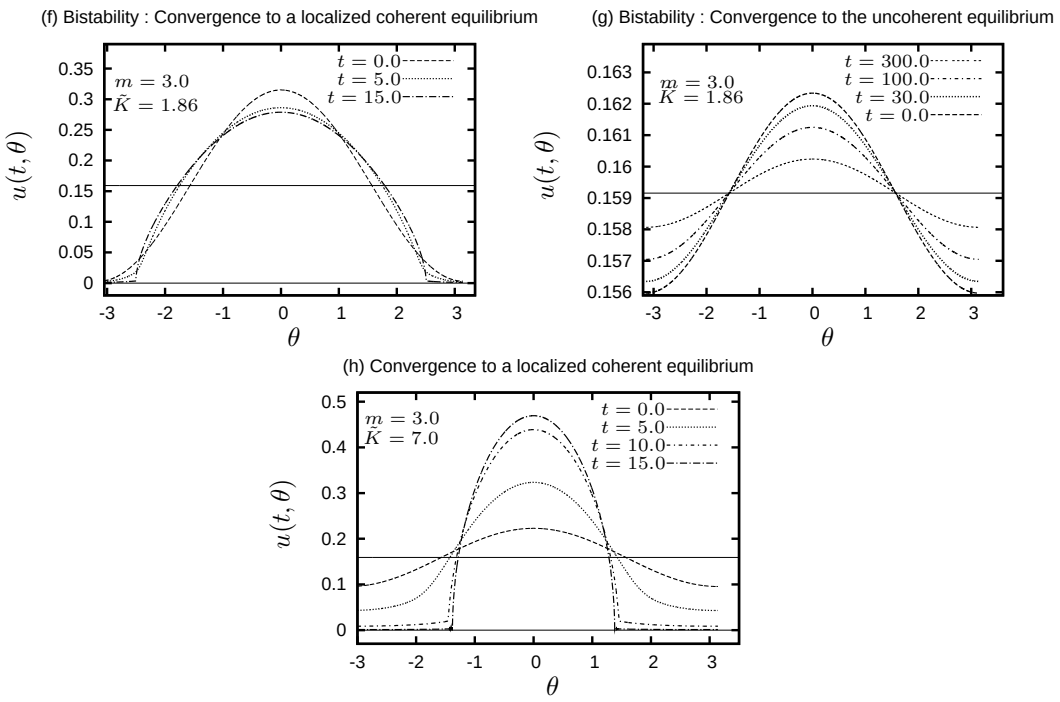

FIGURE 6. Convergence of solutions to equilibria, case $m = 3$. When $\tilde{K} < \min \tilde{K}_m(c)$, solutions converge to the uncoherent equilibrium (region (U) in figure 1). Panels (f) and (g) illustrate the bistability phenomena in region (B) of figure 1 (for $\tilde{K}$ in $]\min \tilde{K}_m(c), 2[$). Using $u_0 = \frac{1}{2\pi} + \frac{x_1}{\pi}\cos(\cdot)$ with $x_1 = 0.5$, panel (f) shows convergence of one solution to the localized coherent equilibria (S_l) when $K = 1.86$, and for the same value of $\tilde{K}$ panel (g) shows that with different initial data ($x_1 = 0.01$) the solution converges to the uncoherent equilibria. When $\tilde{K} > 2$ solutions remain positive and converge to the localized coherent equilibria (S_l) (region (C_l) in figure 1), this is illustrated in panel (h) for $\tilde{K} = 7$. In panels (f) and (h) the solutions have numerically converged at $t = 15.0$ and remain the same for all $t \geq 15.0$. In panel (g) convergence is much slower, using $x_1 = 0.01$ for the initial condition, the solution is still approaching $\frac{1}{2\pi}$ when $t = 300.0$. (Details on numerical methods used here can be found in the appendix.)

bifurcation point. As soon as $\tilde{K} > 2$, the uncoherent steady state $\frac{1}{2\pi}$ is locally unstable (label (P_2) figure 3 panel (a)) and equation (1.1) has a unique localized coherent equilibrium with $x_1 > \frac{1}{2}$ (label (S_l) figure 7 panel (a)).

When $\tilde{K} < \tilde{K}_c$, all solutions converge to the uncoherent equilibrium $\frac{1}{2\pi}$. When $\tilde{K} = 2$ the phase space is foliated by the stable manifolds of the equilibria $u(\cdot) = \frac{1}{2\pi} + \frac{1}{\pi}x_1\cos(\cdot)$ where $0 \leq x_1 \leq \frac{1}{2}$, that is to say: any solution converge to one of those equilibria, which depends on the initial data u_0. Panels (d) and (e) in figure 8 show two solutions of (1.1) for the same value of $\tilde{K} = 2$ and two different initial conditions that converge to two different equilibria of the family (N_p). When $\tilde{K} > 2$, solutions typically converge to the unique (localized) coherent equilibrium (S_l) of (1.1). In figure 8, panel (f) show this convergence phenomena for one solution when $\tilde{K} = 6.0$.

Bifurcation diagrams for $m < 2$, $m = 2$ and $m > 2$ are compared in figure 9. The value of $\tilde{K}$ at which stable and localized equilibria (S_l) appear depends smoothly on m, it equals $\min_c \tilde{K}_m(c)$ when $m < 2$, 2 when $m = 2$ and $\tilde{K}_m(c = 1)$ when $m > 2$. The unstable equilibria (U_p) and (U_l) that exist for $m < 2$ converge to the family of equilibria (N_p) at $m = 2$ and $\tilde{K} = 2$. Similarly the stable and positive equilibria (S_p) that exist when $m > 2$ converge to the family of equilibria (N_p) at $m = 2$ and $\tilde{K} = 2$.

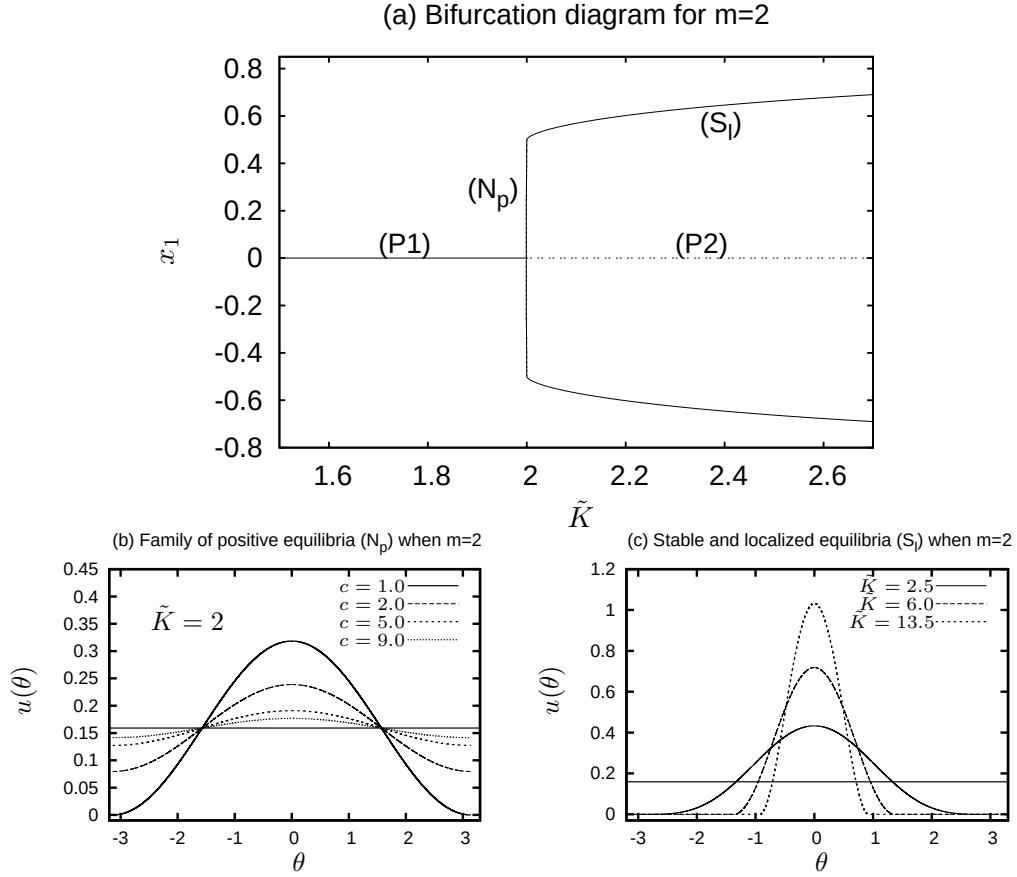

FIGURE 7. Equilibria bifurcation diagram, equilibria of (1.1) and convergence of solutions in case $m = 2$. Panel (a) show the number of equilibria of (1.1) for $0 < \tilde{K} < +\infty$. We see in particular the degenerate pitchfork bifurcation occurring at $\frac{1}{2\pi}$ when $\tilde{K} = 2$. The branch of equilibria that appear at $\tilde{K}_c$ is flat: there is a 1-parameter family of equilibria $u(\cdot) = \frac{1}{2\pi} + \frac{1}{\pi} x_1 \cos(\cdot)$ where $0 \leq x_1 \leq \frac{1}{2}$, connecting $\frac{1}{2\pi}$ (for $x_1 = 0$) to the onset of localized equilibria (for $x_1 = \frac{1}{2}$) (see proposition 4.3). Positive coherent equilibria of his family (N_p) are shown in panel (b), for $\tilde{K} = 2$ and various values of $x_1 = x_1(c)$, and confirm that the equilibrium u converge to $\frac{1}{2\pi}$ has $c \to +\infty$ and $x_1 \to 0$. Panel (c) shows the shape of coherent equilibria (S_l), for various different values of $\tilde{K} > \tilde{K}(c = 1)$ (see proposition (4.2) for analytical formulas for these equilibria). These equilibria are smooth and localized for all $K > 2$, and they converge to a Dirac mass at $\theta = 0$ when $K \to +\infty$. (In panels (b) and (c), the horizontal line represents $\frac{1}{2\pi}$, details on numerical methods used here can be found in the appendix.)

5.4. **Coherence transition when** $m \to +\infty$**.** The limit $m \to +\infty$ is a limit of slow diffusion in (1.1). The bifurcation scenari in the limit m large is illustrated in figure 5.4. The fold bifurcation point $\tilde{K} = \min_c \tilde{K}(c)$ coonverge to the pitchfork bifurcation point $\tilde{K} = 2$, and the interval $\tilde{K} \in [\min_c \tilde{K}(c), 2[$ in which equation (1.1) is bistable vanishes in the large m limit, while the coherent equilibria branch (S_l) converges pointwisely to the unstable uncoherent equilibrium branch (P_2) (see illustrations of these convergence phenomena in figure 5.4).

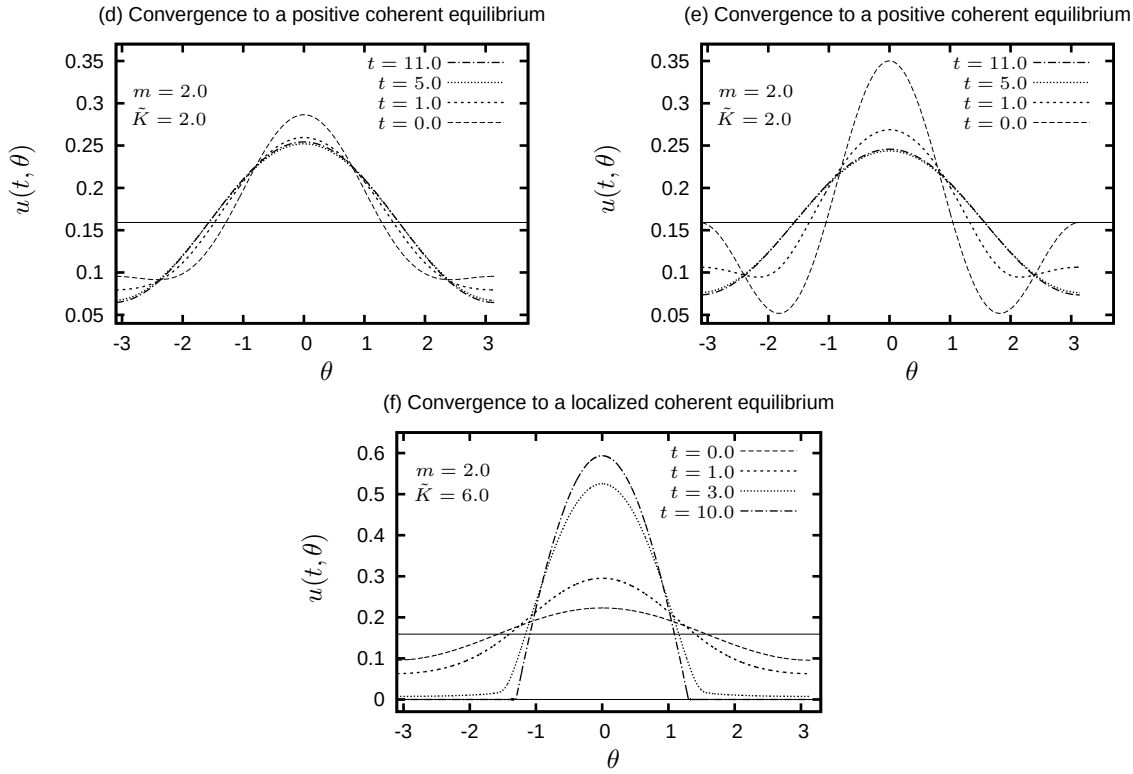

FIGURE 8. Convergence of solutions in case $m = 2$. Panels (d) and (e) show convergence of solutions to different coherent equilibria when $K = 2$. We used $u_0(\theta) = \frac{1}{2\pi} + \frac{a}{\pi}\cos(\theta) + \frac{b}{\pi}\cos(\theta)$ with $a = 0.3$, $b = 0.1$ in (d), and $a = 0.4$, $b = 0.2$ in (e). The solutions converge to $u(\cdot) = \frac{1}{2\pi} + \frac{1}{\pi}x_1\cos(\cdot)$ with $x_1 \approx 0.3$ in (d) and $x_1 \approx 0.36$ in (e). When $\tilde{K} > 2$ solutions remains positive and converge to the localized coherent equilibria (S_l) of (1.1). This is illustrated in panel (f) where the solution has numerically converged at $t = 5.0$ and remains the same for all $t \geq 5.0$. (In panels (d) to (f), the horizontal line represents $\frac{1}{2\pi}$, details on numerical methods used here can be found in the appendix.)

6. Discussion

In this work, we have shown that nonlinear diffusion alters the dynamics of eq (1.1) in two key aspects. One relates to the very shape of coherent equilibria that become localized when advection is strong. The other modification is that for $m > 2$, the transition to coherence scenario is through a subcritical rather than a supercritical pitchfork bifurcation, thereby leading to existence of a multistable regime that has no counter part in the case of linear diffusion. Central to this impact of nonlinear diffusion is the fact that the pitchfork bifurcation for $m = 2$ is highly degenerate and acts as an organizing center. In the following paragraphs we first discuss the implications of this organizing center and then the generality of our results.

Schematically, organizing centers are degenerate bifurcation points where a number of qualitatively distinct regimes come to meet. For eq (1.1) the highly degenerate pitchfork bifurcation taking place at $(\tilde{K}, m) = (2, 2)$ plays this pivotal role. We claim that small perturbations of eq (1.1) at this point can produce arbitrary one-dimensional dynamics of the interval. Indeed, a full continuous interval of equilibria exists at this point. This fact combined with the claim (based upon numerical investigations) that the linearized operator at these equilibria possesses a spectral gap suggest that this equilibria interval is a normally hyperbolic invariant manifold. This property in turn implies that this manifold

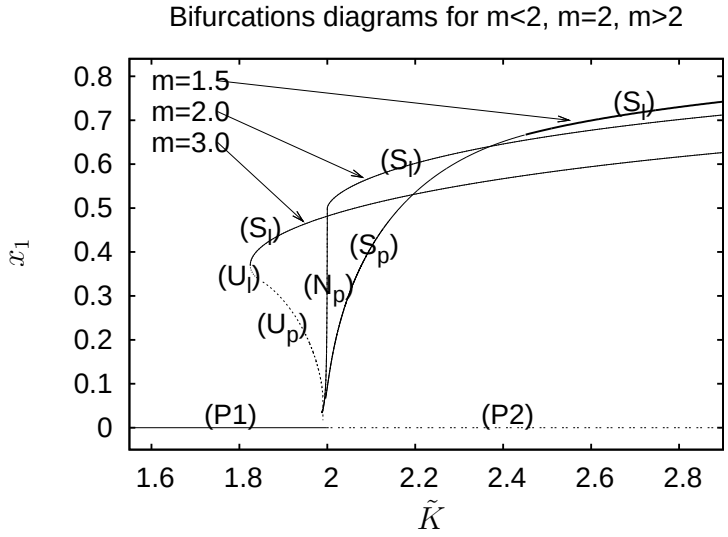

FIGURE 9. Transition in bifurcations diagrams at $m = 2$. The value of $\tilde{K}$ at which stable and localized equilibria (S_l) appear depends smoothly on m, it equals $\min_c \tilde{K}_m(c)$ when $m < 2$, it equals 2 when $m = 2$ and $\tilde{K}_m(c = 1)$ when $m > 2$. The unstable equilibria (U_p) and (U_l) that exist for $m < 2$ converge to the family of equilibria (N_p) at $m = 2$ and $\tilde{K} = 2$. Similarly the stable and positive equilibria (S_p) that exist when $m > 2$ converge to the family of equilibria (N_p) at $m = 2$ and $\tilde{K} = 2$.

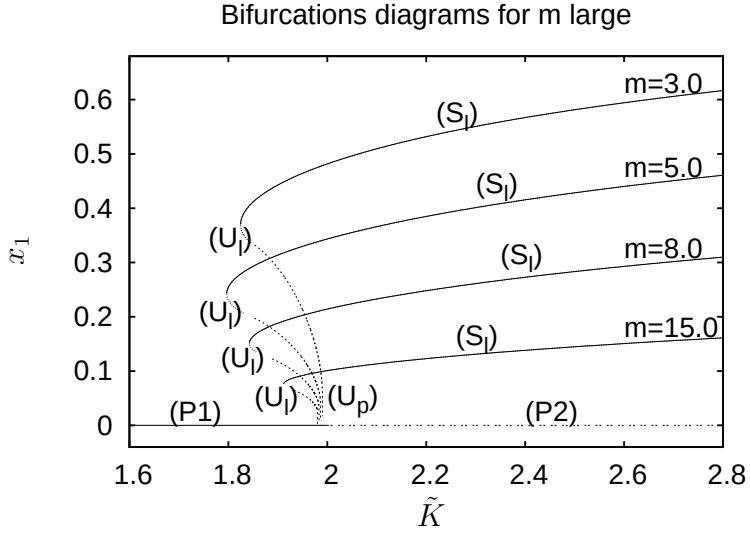

FIGURE 10. Bifurcations diagrams for large m. In the large m limit, the fold bifurcation value $\tilde{K} = \min_c \tilde{K}(c)$ converges to $\tilde{K} = 2$, and the uncoherent equilibria (U_l), (U_p) exist in a vanishing intervall of $\tilde{K}$ (corresponding to the bistability region (B) is figure 1). The coherent localized stable equilibria branch (S_l) converge pointwisely to the uncoherent equilibria branch (P_2).

would persist under small perturbations of eq (1.1). Finally, the fact that dynamics on the equilibria set is trivial allows one to construct ad-hoc small perturbations to reproduce arbitrary dynamics.

A related construction exists for linear diffusion where it has been proved that small perturbations can produce arbitrary dynamics of the circle [21]. While the main arguments, i.e. the existence of a normally hyperbolic contiuum of equilibria are similar in both cases, there exists a main difference. For linear diffusion, the continuum of equilibria does not exist if one considers even solutions, whereas for $m = 2$, it does so. In other words, if we relax the constraint on solutions beeing even, we can expect small perturbations of eq (1.1) to produce arbitrary dynamis on the disk (and not only the interval or the circle). In this sense, our results suggest that the dynamics with nonlinear diffusion are richer than those with linear diffusion and give a precise meaning to this property.

In our work, results were presented for the case where the nonlocal advection term takes on the form of a convolution with a sine function. Here, we discuss extentions of our results to other forms of advection.

For the sake of simplicity, we have restricted our analysis to the coupling term $J * u = \int_{\mathbb{S}} \sin(\cdot - \varphi)u(\varphi)d\varphi$. Results about convergence of equilibria can be extended to more general coupling terms, including the Maier-Saupe potential $J * u = \int_{\mathbb{S}} \sin 2(\cdot - \varphi)u(\varphi)d\varphi$ for example and more general non local convolution with an odd function. In the case of Maier Saupe potential the bifurcation scenario remains very similar to figure 1. The main difference is that coherent equilibria have two maximum on $[-\pi, \pi]$, and localized coherent equilibria have non-connected support of the form $]\pi - \epsilon, \pi + \epsilon[\cup] - \epsilon, \epsilon[$.

Polynomial advecting terms have been considered in the context of Keller-Segel model with degenerate diffusion for example see [39, 38, 40] . The corresponding equations

$$\begin{cases} \partial_t u &= \partial_\theta^2(u^m) + \partial_\theta \left(u^q J * u\right), & t > 0,\, \theta \in [0, 2\pi], \\ u(0,\theta) &= u_0(\theta) & \theta \in [0, 2\pi], \\ u(t,0) &= u(t, 2\pi) & t \geq 0, \\ \partial_\theta u(t,0) &= \partial_\theta u(t, 2\pi) & t \geq 0, \end{cases} \tag{6.1}$$

with $1 \leq q < m$ can be treated as the case $q = 1$ and the bifurcation scenari are the same, with value m changed to $m - (q - 1)$. Here we simply show that proposition 4.2 on the equilibria set of (1.1) can be directly extended to the following corollary

Corollary. *Let u be a stationary solution of (6.1) with $1 \leq q < m$. Then we have*

$$u^{m-q}(\theta) = \frac{m-q}{m} K x_1 \left[\cos(\theta) + c\right]_+$$

where x_1 and K are given by

$$x_1 = \frac{J_{m-(q-1)}}{I_{m-(q-1)}},\ K = \frac{m}{m-q}\frac{1}{x_1}\frac{1}{I_{m-(q-1)}^{m-q}} = \frac{m}{m-q}\frac{1}{J_{m-(q-1)}}\frac{1}{I_{m-(q-1)}^{m-q-1}}$$

for $c \in]-1, +\infty[$, where I_m and J_m are defined as in proposition 4.2.

Acknowledgments

Xavier Pellegrin would like to thank Michael Goldman for interesting discussions on gradient flows.

Appendix

Figure 3 panels (a) to (c), figure 7 panels (a) to (c), and figure 5 panels (a) to (e), were made using formulas (4.4) and (4.6) that give x_1, $\tilde{K}$ and the coherent equilibria u as functions of c. The functions $I_m(c)$ and $J_m(c)$ were approximated by the classical trapezoidal rule with space discretization $\Delta_\theta = 10^{-3}$ for $c \in]-1, 2[$ with discretization $\Delta_c = 10^{-2}$. The coherent equilibria are stable exactly when $c < 1$ and $\tilde{K} > \min \tilde{K}(c)$. The coherent equilibria are localized exactly when $c < 1$. The bifurcation diagram in a neighborhood of $\tilde{K} = 2$ and $x_1 = 0$ is obtained in the limit $c \to +\infty$. Since we have proven analytically that $\tilde{K} - 2 = O(x_1^2)$ in that limit, the have extended the curves obtained with $c \in]-1, 2[$ by straight

lines for $c > 2$. Meanwhile the values $\min_{c\in]-1,1[} \tilde{K}(c)$ were recorded for each m, and then used to draw the border between regions (U) and (B) in figure 1. In the same figure the borders between regions (B_l) and (B_p) and regions (C_l) and (C_p) were obtained for $\tilde{K}(c = 1)$.

Simulations of solutions of (1.1) shown in figures in the main text have been done using a finite difference scheme to discretize the diffusion operator

$$\partial_\theta^2 u^m(\theta) \approx \frac{u^m(\theta + \Delta_\theta) + u^m(\theta - \Delta_\theta) - 2u^m(\theta)}{(\Delta_\theta)^2},$$

a symmetric scheme for the advection term

$$\partial_\theta(uJ * u) \approx Kx_1 \frac{u(\theta + \Delta_\theta)\sin(\theta + \Delta_\theta) - u(\theta - \Delta_\theta)\sin(\theta - \Delta_\theta)}{2\Delta_\theta}$$

and a explicit Euler scheme for the time derivative. Unless something else is explicitly mentioned, we have used the initial condition $u_0(\theta) = \frac{1}{2\pi} + \frac{0.2}{\pi}\cos(\theta)$. We mention that the scheme slightly unstabilize the uncoherent equilibria even when $\tilde{K} < \tilde{K}_c$. It also increases diffusion phenomena and induces some numerical instabilities at the border of the support of solutions when this support is strictly included in $]0, 2\pi[$. Numerical results have been checked using $(\Delta_\theta, \Delta_t) = (2.0\,10^{-2}, 10^{-4})$ and $(\Delta_\theta, \Delta_t) = (2.0\,10^{-3}, 10^{-6})$, convergence has been checked when $\Delta_\theta, \Delta_t \to 0$, and the convergence rate is $O(\Delta_\theta) + O(\Delta_t) + O(\frac{(\Delta_\theta)^2}{\Delta_t})$.

References

1. Juan A. Acebrón, L. L. Bonilla, Conrad J. Pérez Vicente, Félix Ritort, and Renato Spigler, *The kuramoto model: A simple paradigm for synchronization phenomena*, Rev. Mod. Phys. **77** (2005), no. 1, 137–185.
2. D. G. Aronson, *Regularity propeties of flows through porous media*, SIAM J. Appl. Math. **17** (1969), 461–467. MR 0247303 (40 #571)
3. ———, *Regularity properties of flows through porous media: A counterexample.*, SIAM J. Appl. Math. **19** (1970), 299–307. MR 0265774 (42 #683)
4. ———, *Regularity properties of flows through porous media: The interface.*, Arch. Rational Mech. Anal. **37** (1970), 1–10. MR 0255996 (41 #656)
5. Donald Aronson, Michael G. Crandall, and L. A. Peletier, *Stabilization of solutions of a degenerate nonlinear diffusion problem*, Nonlinear Anal. **6** (1982), no. 10, 1001–1022. MR 678053 (84j:35099)
6. Jacob Bear, *Modeling transport phenomena in porous media*, Environmental studies (Minneapolis, MN, 1992), IMA Vol. Math. Appl., vol. 79, Springer, New York, 1996, pp. 27–63. MR 1417048
7. Lorenzo Bertini, Giambattista Giacomin, and Khashayar Pakdaman, *Dynamical aspects of mean field plane rotators and the Kuramoto model*, J. Stat. Phys. **138** (2010), no. 1-3, 270–290. MR 2594897
8. M. Bodnar and J. J. L. Velazquez, *Derivation of macroscopic equations for individual cell-based models: a formal approach*, Math. Methods Appl. Sci. **28** (2005), no. 15, 1757–1779. MR 2166611 (2006f:60091)
9. ———, *An integro-differential equation arising as a limit of individual cell-based models*, J. Differential Equations **222** (2006), no. 2, 341–380. MR 2208049 (2006k:45028)
10. J. Buckmaster, *Viscous sheets advancing over dry beds*, J. Fluid Mech. **81** (1977), no. 4, 735–756. MR 0455812 (56 #14046)
11. M. Burger, M. Di Francesco, and M. Franek, *Stationary states of quadratic diffusion equations with long-range attraction*, ArXiv e-prints (2011).
12. Martin Burger, Vincenzo Capasso, and Daniela Morale, *On an aggregation model with long and short range interactions*, Nonlinear Analysis: Real World Applications **8** (2007), no. 3, 939 – 958.
13. Martin Burger and Marco Di Francesco, *Large time behavior of nonlocal aggregation models with nonlinear diffusion*, Networks and Heterogeneous Media **3** (2008), 749–785.
14. J. Carrillo and J. Vázquez, *Asymptotic complexity in filtration equations*, Journal of Evolution Equations **7** (2007), 471–495, 10.1007/s00028-006-0298-z.
15. Peter Constantin, Edriss S. Titi, and Jesenko Vukadinovic, *Dissipativity and Gevrey regularity of a Smoluchowski equation*, Indiana Univ. Math. J. **54** (2005), no. 4, 949–969. MR 2164412 (2006e:35162)
16. Peter Constantin and Jesenko Vukadinovic, *Note on the number of steady states for a two-dimensional Smoluchowski equation*, Nonlinearity **18** (2005), no. 1, 441–443. MR 2109485 (2005h:82121)
17. John D. Crawford and K. T. R. Davies, *Synchronization of globally coupled phase oscillators: singularities and scaling for general couplings*, Physica D: Nonlinear Phenomena **125** (1999), no. 1-2, 1 – 46.

18. Weibing Deng, Zhiwen Duan, and Chunhong Xie, *The blow-up rate for a degenerate parabolic equation with a non-local source*, J. Math. Anal. Appl. **264** (2001), no. 2, 577–597. MR 1876751 (2002i:35107)
19. Jesus Ildefonso Diaz and Robert Kersner, *On a nonlinear degenerate parabolic equation in infiltration or evaporation through a porous medium*, J. Differential Equations **69** (1987), no. 3, 368–403. MR 903393 (88i:35088)
20. Giambattista Giacomin, Khashayar Pakdaman, and Xavier Pellegrin, *Global attractor and asymptotic dynamics in the kuramoto model for coupled noisy phase oscillators*, ArXiv e-prints (2011).
21. Giambattista Giacomin, Khashayar Pakdaman, Xavier Pellegrin, and Christophe Poquet, *Transitions in generalized active rotators systems : invariant hyperbolic manifold approach*, arXiv:1106.0758v2 (2011).
22. B. H. Gilding, *A nonlinear degenerate parabolic equation*, Ann. Scuola Norm. Sup. Pisa Cl. Sci. (4) **4** (1977), no. 3, 393–432. MR 0509720 (58 #23077)
23. ———, *Improved theory for a nonlinear degenerate parabolic equation*, Ann. Scuola Norm. Sup. Pisa Cl. Sci. (4) **16** (1989), no. 2, 165–224. MR 1041895 (91h:35182a)
24. Morton E. Gurtin and Richard C. MacCamy, *On the diffusion of biological populations*, Math. Biosci. **33** (1977), no. 1-2, 35–49. MR 0682594 (58 #33147)
25. Michel Langlais and Daniel Phillips, *Stabilization of solutions of nonlinear and degenerate evolution equations*, Nonlinear Anal. **9** (1985), no. 4, 321–333. MR 783581 (87c:35018)
26. Thomas Laurent, *Local and global existence for an aggregation equation*, Comm. Partial Differential Equations **32** (2007), no. 10-12, 1941–1964. MR 2372494 (2008k:35475)
27. D. Li and X. Zhang, *On a nonlocal aggregation model with nonlinear diffusion*, ArXiv e-prints (2009).
28. Chong Luo, Hui Zhang, and Pingwen Zhang, *The structure of equilibrium solutions of the one-dimensional doi equation*, Nonlinearity **18** (2005), no. 1, 379.
29. Alexander Mogilner and Leah Edelstein-Keshet, *A non-local model for a swarm*, J. Math. Biol. **38** (1999), no. 6, 534–570. MR 1698215 (2000e:92058)
30. Daniela Morale, Vincenzo Capasso, and Karl Oelschläger, *An interacting particle system modelling aggregation behavior: from individuals to populations*, J. Math. Biol. **50** (2005), no. 1, 49–66. MR 2117406 (2005i:92022)
31. Toshitaka Nagai and Masayasu Mimura, *Asymptotic behavior for a nonlinear degenerate diffusion equation in population dynamics*, SIAM J. Appl. Math. **43** (1983), no. 3, 449–464. MR 700524 (85c:35046)
32. Akira Okubo, *Diffusion and ecological problems: mathematical models*, Biomathematics, vol. 10, Springer-Verlag, Berlin, 1980, An extended version of the Japanese edition, ıt Ecology and diffusion, Translated by G. N. Parker. MR 572962 (81i:92025)
33. Felix Otto, *The geometry of dissipative evolution equations: the porous medium equation*, Comm. Partial Differential Equations **26** (2001), no. 1-2, 101–174. MR 1842429 (2002j:35180)
34. Felix Otto and Michael Westdickenberg, *Eulerian calculus for the contraction in the Wasserstein distance*, SIAM J. Math. Anal. **37** (2005), no. 4, 1227–1255 (electronic). MR 2192294 (2007c:28003)
35. H. Silver, N. E. Frankel, and B. W. Ninham, *A class of mean field models*, Journal of Mathematical Physics **13** (1972), no. 4, 468–474.
36. Steven H. Strogatz, *From Kuramoto to Crawford: exploring the onset of synchronization in populations of coupled oscillators*, Phys. D **143** (2000), no. 1-4, 1–20, Bifurcations, patterns and symmetry. MR 1783382 (2001g:82008)
37. Steven H. Strogatz and Renato E. Mirollo, *Stability of incoherence in a population of coupled oscillators*, J. Statist. Phys. **63** (1991), no. 3-4, 613–635. MR 1115806 (92h:34077)
38. Y. Sugiyama, *Finite speed of propagation in 1-D degenerate Keller-Segel system*, ArXiv e-prints (2009).
39. Yoshie Sugiyama, *Global existence in sub-critical cases and finite time blow-up in super-critical cases to degenerate Keller-Segel systems*, Differential Integral Equations **19** (2006), no. 8, 841–876. MR 2263432 (2008h:35134)
40. ———, *Interfaces for 1-D degenerate Keller-Segel systems*, J. Evol. Equ. **9** (2009), no. 1, 123–142. MR 2501355 (2010b:35230)
41. Chad Topaz, Andrea Bertozzi, and Mark Lewis, *A nonlocal continuum model for biological aggregation*, Bulletin of Mathematical Biology **68** (2006), 1601–1623, 10.1007/s11538-006-9088-6.
42. Juan Luis Vázquez, *The porous medium equation*, Oxford Mathematical Monographs, The Clarendon Press Oxford University Press, Oxford, 2007, Mathematical theory. MR 2286292 (2008e:35003)
43. Jesenko Vukadinovic, *Inertial manifolds for a Smoluchowski equation on a circle*, Nonlinearity **21** (2008), no. 7, 1533–1545. MR 2425333 (2009i:37197)

Institut Jacques Monod, Université Paris 7–Denis Diderot, Bat. Buffon, 15 rue Héléne Brion - 75013 Paris, France

Institut Jacques Monod, Université Paris 7–Denis Diderot, Bat. Buffon, 15 rue Héléne Brion - 75013 Paris, France